

Localization in weakly coupled planes and weakly coupled wires

I. Zambetaki

Research Center of Crete and Department of Physics, P. O. Box 1527, 71110 Heraklion, Crete, Greece

Qiming Li

Ames Laboratory and Department of Physics and Astronomy, Iowa State University, Ames, Iowa 50011

E. N. Economou

Research Center of Crete and Department of Physics, P. O. Box 1527, 71110 Heraklion, Crete, Greece

C. M. Soukoulis

*Research Center of Crete and Department of Physics, P. O. Box 1527, 71110 Heraklion, Crete, Greece
and Ames Laboratory and Department of Physics and Astronomy, Iowa State University, Ames, Iowa 50011*

(Received 2 May 1997)

We investigate the localization behavior of the Anderson model with anisotropic hopping integral t for weakly coupled planes and weakly coupled chains both numerically with the transfer matrix method and analytically within the self-consistent theory of localization. It is found that the mobility edge is independent of the propagating direction. However, the correlation ξ (localization L_c) length in the extended (localized) side of the transition can be very different for the two directions. We find that $\xi^{\parallel} = t^2 \xi^{\perp}$ and $L_c^{\perp} = t L_c^{\parallel}$, in agreement with the scaling theory of localization. We discuss how this can possibly explain the transport properties of high- T_c materials. The critical disorder W_c is found to vary as $t^{1/4}$ for weakly coupled planes and as $t^{1/2}$ for weakly coupled chains. A discrepancy with the predictions of a diagrammatic analysis on the conductance ratio is discussed. [S0163-1829(97)03544-3]

I. INTRODUCTION

The problem of Anderson localization in anisotropic systems has attracted considerable attention¹⁻⁵ in recent years, largely due to the fact that the high T_c superconductors are highly anisotropic. Transport in the normal state is metallic in the x - y plane, but appears semiconductorlike on the z axis.⁶ The nature of the z -axis transport in high- T_c materials is still controversial and its understanding may have important consequences for the theories of the normal and the superconducting state. This paradoxical property has prompted the proposal⁷ that a high- T_c material in the normal state is actually an insulator, appearing metallic only because the inelastic length in the plane is less than the localization length. It has also been argued^{2,6} that a negative dp/dT in the z direction alone may signify anisotropic localization, with a metal-insulator transition depending on the propagating direction, in direct contradiction to the predictions of the scaling theory of localization.⁸ A recent diagrammatic calculation¹ lent support to such a claim. Previous diagrammatic analysis,⁹ however, led to the conclusion that the scaling property in anisotropic systems remains the same as that of the isotropic systems with a simple substitution of the conductance by its geometric mean. Given the perturbative nature of all the previous work, it is important to carefully study the localization behavior of disordered anisotropic systems with reliable numerical techniques and to determine whether the scaling theory is valid for highly anisotropic systems.⁸⁻¹¹

In the present work, we have systematically studied the localization properties of a three-dimensional disordered an-

isotropic system and our analysis on sufficiently large systems has revealed the following properties.

(i) The metal-insulator transition is independent of the propagating direction.

(ii) At the critical point, the geometric mean of the ratios of the finite-size localization lengths to the width of the bar is independent of the anisotropy. This remarkable relation might underline the conformal invariance property at the Anderson transition.^{12,13}

(iii) The critical disorder W_c seems to vary with the anisotropy t as $t^{1/4}$, in disagreement with the expected logarithmic dependence. Our diagrammatic theory of the anisotropic localization can provide an explanation for this remarkable relation.

(iv) The critical exponents for the correlation and localization length for both propagating directions are equal to that of the isotropic system.

(v) The difference between the correlation lengths in the different propagating directions may possibly explain the normal state transport properties of the high- T_c materials.

We have also studied the localization behavior of weakly coupled chains, which simulate the one-dimensional (1D) to 3D continuous transition. We also find that the metal-insulator transition is independent of the propagating direction and that, at the critical point, the geometric mean of the λ_M/M for the different directions is constant, independent of the anisotropy. The critical disorder W_c is found to behave as $t^{1/2}$, in agreement with previous studies and with the results of the coherent potential approximation.

We used the transfer-matrix and finite-size scaling techniques to calculate both the conductance and the localization

length. In Sec. II we describe the model and the numerical techniques we used, in Sec. III we present and discuss our numerical results, in Sec. IV the transport high- T_c materials are discussed, in Sec. V we present our analytical work and compare with numerical results, and in Sec. VI we summarize the conclusions of this work.

II. MODEL AND NUMERICAL TECHNIQUES

We are considering a general three-dimensional tight-binding Hamiltonian on a simple cubic lattice with one orbital per lattice site. The corresponding difference equation for the amplitudes of the wave function, $c_{l,n,m}$, written for a bar of length L and square cross section $M \times M$, takes the form

$$\begin{aligned} (E - \epsilon_{l,n,m})c_{l,n,m} = & t_x(c_{l-1,n,m} + c_{l+1,n,m}) \\ & + t_y(c_{l,n-1,m} + c_{l,n+1,m}) \\ & + t_z(c_{l,n,m-1} + c_{l,n,m+1}), \end{aligned} \quad (1)$$

where a lattice site is denoted by the set (l,n,m) , with $l=1,2,\dots,L$ and $n,m=1,2,\dots,M$. The lattice spacing is taken equal to unity, while the diagonal random site energies $\epsilon_{l,n,m}$ associated with every lattice site (l,n,m) are chosen from a box probability distribution of mean zero and width W . We define the z direction as the propagating direction, so t_z is the hopping matrix element along the propagating direction, while t_x and t_y are the hopping integrals in the x and y directions, respectively. In the simple cubic lattice of our tight-binding model, the hopping integrals are nonzero only between nearest-neighbor sites and depend on directions in general, $t_x \neq t_y \neq t_z$. We normalize all the energies by the largest hopping integral, so all the parameters t_x , t_y and t_z take values between 0 and 1.

In this work we study the cases that t_x is equal to t_z or t_y . When $t_x = t_z = 1$ or $t_x = t_y = 1$ the system consists of a set of coupled planes and the propagation takes place parallel or perpendicular to the planes, respectively. When $t_x = t_z < 1$ or $t_x = t_y < 1$, the system consists of a set of coupled chains and the propagation takes place perpendicular or parallel to the chains, respectively. As a convention, we assign the direction with the large and small hopping integral as the parallel (\parallel) and the perpendicular (\perp) direction, respectively. We define t as the ratio of the small hopping integral over the large one, so t measures the anisotropy ratio and takes values between 0 and 1.

First, we treat this problem of Anderson transition using the transfer-matrix technique,¹⁴ combined with the one-parameter scaling conjecture. Our model [described with Eq. (1)], is particularly suitable for the transfer-matrix approach since the linear lattice of size L is exceedingly large (by orders of magnitude) in comparison to the size M in the perpendicular directions. In this representation, the evolution of the state is described by a product of transfer matrices $Q_L = \prod_{l=1}^L T_l$. For each l , the transfer matrix T_l connects the amplitudes $c_{l-1,n,m}, c_{l,n,m}$ with the amplitudes $c_{l,n,m}, c_{l+1,n,m}$ ($n, m = 1, 2, \dots, M$). The product matrix Q_L satisfies the theorem of Oseledec,¹⁵ namely, that there exists a limiting matrix

$$\Gamma = \lim_{L \rightarrow \infty} (Q_L Q_L^\dagger)^{1/2L}, \quad (2)$$

with eigenvalues $\exp(\gamma_j)$, where γ_j , $j=1,2,\dots,2M^2$ denotes the characteristic Lyapunov exponents of Q_L . The M^2 Lyapunov exponents of Q_L are positive ($0 < \gamma_1 < \gamma_2 < \dots < \gamma_{M^2}$), while the negative ones are equal to $-\gamma_1, -\gamma_2, \dots, -\gamma_{M^2}$. The smallest of the M^2 positive Lyapunov exponents γ_1 eventually determines the slowest possible exponential increase of the state for $L \rightarrow \infty$. Therefore, it can be identified with the inverse of the longest exponential localization length λ_M ($\lambda_M = \gamma_1^{-1}$) in the quasi-1D system of cross-sectional area M^2 .

Scaling is made possible by varying the perpendicular size parameter M . According to the one-parameter scaling theory, for given M the λ_M/M should be a function of M/λ only for any anisotropy hopping parameter t , disorder value W , and electronic energy state E . The M -independent characteristic length λ equals the localization length $\lambda \equiv \lim_{M \rightarrow \infty} \lambda_M$ as $M \rightarrow \infty$ (if the states are localized) and characterizes the extent of the largest-amplitude fluctuation (if the states are extended). For $W > W_c$ the ratio λ_M/M is expected to fall with increasing M , while for $W < W_c$ it should instead rise. For $W = W_c$ the ratio λ_M/M has a value independent of M and this behavior defines the Anderson transition point. We make the further assumption that the scaling parameter $\lambda(E, W, t)$ diverges as $W \rightarrow W_c$ with a power law $\lambda \sim |W - W_c|^{-\nu}$. This defines the exponent ν , which is $\nu \approx 1.3$ for the simple cubic isotropic system.

The Lyapunov exponents may be used directly to calculate the conductance g of a quasi-1D system¹⁶ (in units of e^2/h)

$$g = \sum_{j=1}^{M^2} \frac{2}{\cosh^2(\gamma_j L)}. \quad (3)$$

Another way¹⁴ to calculate the conductance g of a $M \times M \times M$ cube is from the multichannel Landauer formula¹⁷

$$G(M) = \frac{e^2}{h} \text{Tr}(t^\dagger t), \quad (4)$$

where t is the transmission matrix. The behavior of the conductance g vs M can determine the localization properties of the system similarly to λ_M/M within the localization length λ_M calculations. For localized states ($W > W_c$), g is expected to fall with increasing M ; for extended states ($W < W_c$), g should rise; for $W = W_c$, g is independent of M and this defines the Anderson transition point.

III. NUMERICAL RESULTS AND DISCUSSION

Using the numerical techniques and finite-size scaling assumption described above, we studied the Anderson transition in three-dimensional anisotropic systems. In Fig. 1 we present our numerical results for the conductance $g = G/e^2/h$ versus M , calculated by the Landauer formula given by Eq. (4), for a system of weakly coupled planes. The calculation is for the center of the band $E = 0$ and the size of the cubic system $M \times M \times M$ that is used is $M = 5, \dots, 20$. Because of

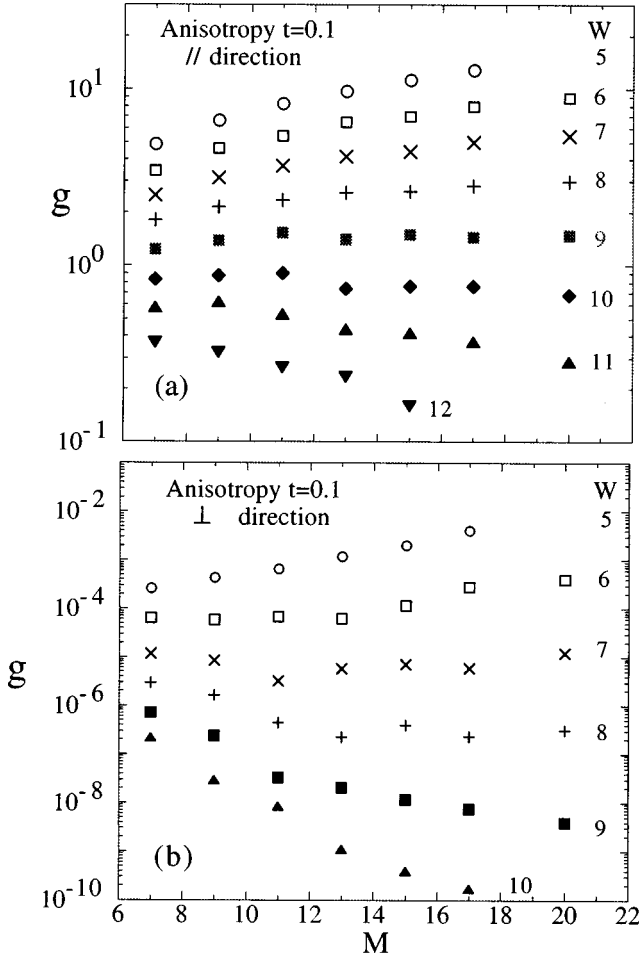


FIG. 1. Conductance g plotted as a function of M for $E=0$, $t=0.1$, and various values of disorder W , for both propagating directions. The calculation is done by the multichannel Landauer formula (4) for a cube of size $M \times M \times M$.

the non-self-averaging nature of finite-size systems, an average over many random configurations (up to 500 for the $M=20$ case) must be taken to suppress the large fluctuations. The anisotropy ratio is $t=0.1$ and we present results for both propagating directions. Notice that for propagation perpendicular to the planes and for disorder close to the critical point (e.g., $W=8$) the conductance g decreases for small M , but it increases for larger system size M . If we only use the numerical results of systems with sites up to $M=11$, we would derive the result that the critical disorder in the perpendicular direction is different, much lower in fact than the value $W_c=8.5$, which is the critical disorder for propagation along the parallel direction. However, if we use large enough systems, which are difficult to obtain numerically ($M \geq 13$ for this value of anisotropy $t=0.1$), we clearly see that the critical disorder has approximately the same value $W_c \approx 8.5$ in both directions. This result is also supported by the results to be presented later, for λ_M/M versus M and the behavior of correlation and localization length versus disorder. The critical conductance in the two directions at $t=0.1$ is approximately $g_c^\perp \approx 10^{-7} g_c^\parallel$, which is a much stronger varia-

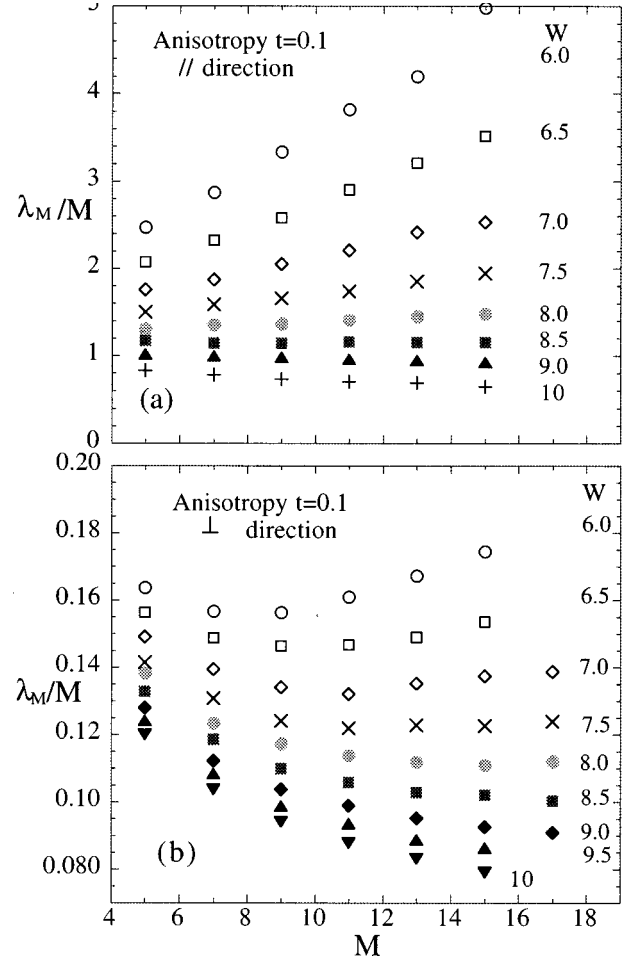


FIG. 2. We plot λ_M/M , as calculated through the transfer matrix techniques, vs M for $E=0$, $t=0.1$, and various values of disorder W , for both propagating directions.

tion than the $g^\perp \approx t^2 g^\parallel$, predicted by the diagrammatic analysis⁹ of the anisotropic model. This may be an indication of the existence of high-order corrections to the conductivity that is not simply proportional to the bare conductivity. This point will be discussed in more detail below.

Using the transfer-matrix technique for a long bar of length L and width $M \times M$, we obtained the localization lengths λ_M for both directions at the center of the band $E=0$. These results are presented in Fig. 2. The maximum width M of the bars that we used was 17, which is the largest width ever used for this kind of calculation. The length L we used was at least 5000 and an average over 20 different samples was taken in order to estimate the error in the calculation of the longest localization length λ_M . The error bars of the numerical data for λ_M/M are less than the size of the printed points. In the figures the error bars are not explicitly drawn.

The results in Fig. 2 clearly support the findings that the critical disorder seems to be $W_c \approx 8.5$ for both propagating directions. The critical disorder is defined by an M independent λ_M/M . Notice again that if only sizes $M \leq 11$ were used, which are appropriate in the isotropic case, one would then have erroneously concluded that $W_c^\parallel > W_c^\perp$.

In order to be able to extrapolate to the infinite system size ($M \rightarrow \infty$) it is necessary to investigate the scaling behavior of λ_M/M . It was found numerically that the function λ_M/M obeys a simple scaling relation of the form

$$\frac{\lambda_M}{M} = f\left(\frac{\lambda}{M}\right). \quad (5)$$

This is correct for both directions. The quantity λ is the localization length L_c for the localized regime and λ is the correlation length ξ for the extended regime. The quantities ξ and L_c are calculated by the relations

$$\frac{\lambda_M}{M} = a + \frac{M}{\xi}, \quad (6)$$

$$\frac{M}{\lambda_M} = a^{-1} + \frac{M}{L_c} \quad (7)$$

for extended and localized states, respectively. In cases where it is difficult to obtain reliable values for ξ and L_c from Eqs. (6) and (7), we use the fact that λ_M/M has to follow the scaling relation given by Eq. (5). In these cases, ξ and L_c are chosen in such a way that all the raw data of λ_M/M follow a universal curve. Of course, at the end we make sure that the dependence of ξ and L_c on disorder W is monotonic. The scaling function $f(x)$ for both directions behaves as $1/x$ in the limit $x \rightarrow 0$ for extended states, while for localized states $f(x) \sim x$ in the limit $x \rightarrow 0$. This is clearly seen in Fig. 3, where the scaling functions for both directions are shown.

From Fig. 3 we see that close to the critical transition point λ_M/M tends to a critical value $\Lambda_c \equiv (\lambda_M/M)_c$, which for the parallel propagating direction is $\Lambda_c^{\parallel} = 1.2$ and for the perpendicular propagating direction $\Lambda_c^{\perp} = 0.12$. The important point here is that for a given energy E and anisotropy ratio t , the critical value $(\lambda_M/M)_c$ depends on the propagating directions. The values of Λ_c we obtained for $E=0$ and anisotropy $t=0.1$ suggest that $\Lambda_c^{\perp} = t\Lambda_c^{\parallel}$. This formula is indeed correct for all t 's we have examined, for weakly coupled planes, and this is shown in Fig. 4. Notice that for weakly coupled chains $\Lambda_c^{\perp} \neq t\Lambda_c^{\parallel}$ it rather looks like $\Lambda_c^{\perp} \approx t^{3/2}\Lambda_c^{\parallel}$, but we have no theoretical understanding of this relation. Since there is this strong dependence of $(\lambda_M/M)_c$ on the anisotropy parameters we cannot use the value of $(\lambda_M/M)_c = 0.6$ (which is the value for the isotropic 3D system) as a criterion for the transition point of Anderson localization. Another important relation that we were able to obtain is that the geometric mean of the different critical values Λ_c in the different directions is independent of the anisotropy t . We derived that

$$(\Lambda_c^x \Lambda_c^y \Lambda_c^z)^{1/3} = 0.6. \quad (8)$$

Our results are shown in Fig. 5 for both plane and wire coupling. In the case of weakly coupled planes, Eq. (8) becomes $[(\Lambda_c^{\perp})^2 \Lambda_c^{\parallel}]^{1/3} = 0.6$. This relation may have important consequences for the existence of conformal invariance at the critical point of the Anderson localization problem.^{12,13} Another more plausible explanation which is based on scal-

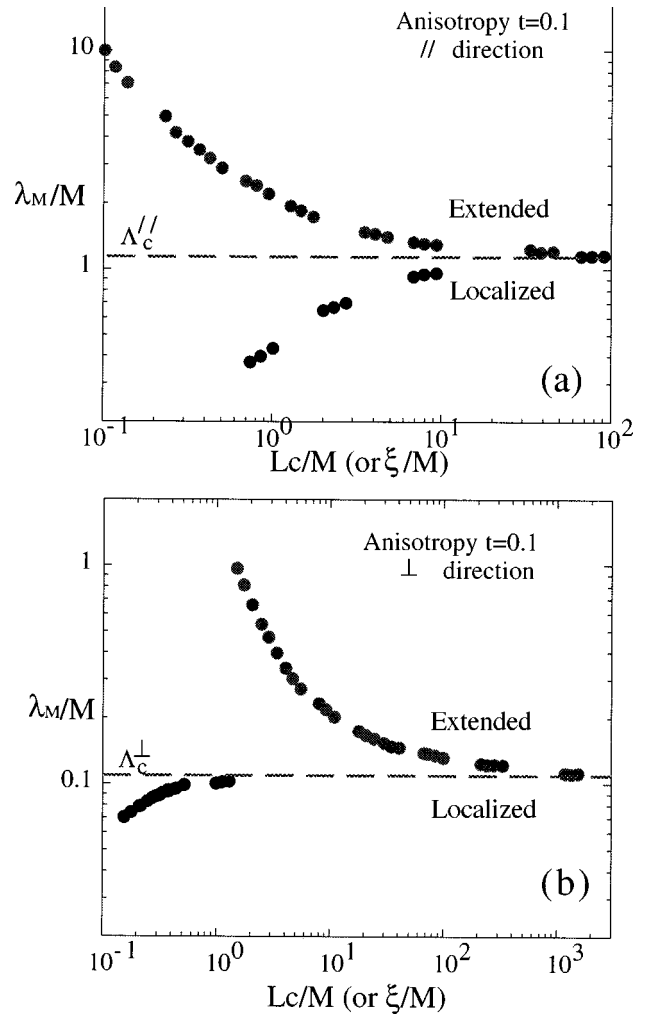


FIG. 3. Renormalized localization length λ_M/M vs ξ/M (or L_c/M) for various values of disorder W for $E=0$ and $t=0.1$ for the (a) parallel and (b) perpendicular propagating direction. There are two branches in the universal curve, the upper one corresponding to extended states and ξ/M and the lower one to localized states and L_c/M . Thus mobility edges exist for both propagations and $\Lambda_c^{\perp} \approx t\Lambda_c^{\parallel}$.

ing arguments,¹⁸ is that $\lambda_M^{\parallel}/M = (\xi^{\parallel}/\xi^{\perp})f(M/\xi^{\perp})$ for the parallel direction and two corresponding expressions for the perpendicular directions. At the critical point, the geometric mean of λ_M/M is a constant, equal to the isotropic value of 0.6.

In Fig. 6 the scaling parameters ξ and λ for the center of the band and for anisotropy ratio $t=0.1$ are shown, as functions of the disorder W , for both directions. We see that in the extended regime where $W < W_c$, $\xi^{\perp} > \xi^{\parallel}$. For example, at $W=5$, $\xi^{\perp} = 100$ and $\xi^{\parallel} \approx 1.5$, in units of the lattice constant, which has been taken to be one. In the localized regime where $W > W_c$, $L_c^{\parallel} > L_c^{\perp}$. For example, at $W=10$, $L_c^{\parallel} \approx 5$ and $L_c^{\perp} \approx 55$. Our numerical results approximately follow the theoretical predictions¹⁹ that $\xi^{\parallel} = t^2 \xi^{\perp}$ and $L_c^{\perp} = tL_c^{\parallel}$. The t dependence of the ratio of the localization lengths along the two propagating directions also explains why $\Lambda_c^{\perp} = t\Lambda_c^{\parallel}$ for weakly coupled planes, as shown in Fig. 4. $\Lambda_c = (\lambda_M/M)_c$

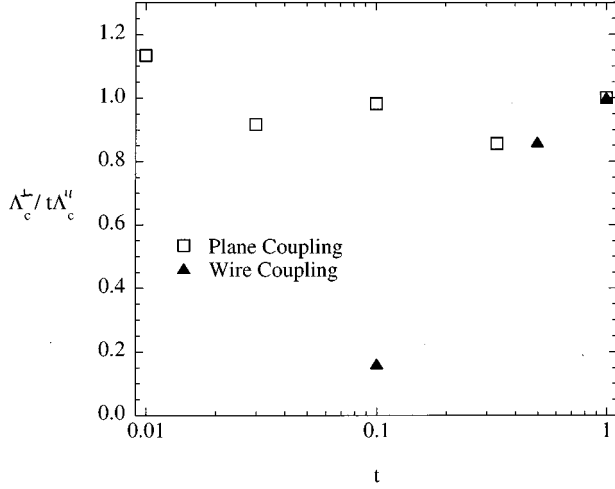


FIG. 4. Ratio $\Lambda_c^\perp / t \Lambda_c^\parallel$ vs the anisotropy t , for plane and wire coupling. Notice that $\Lambda_c^\perp = t \Lambda_c^\parallel$ is obeyed only for weakly coupled planes.

and since λ_M is a length along the parallel direction, it has to scale as the localization length and therefore has the same t dependence.

Let us discuss now the ratio of the conductances along the two propagating directions. As is clearly seen from Fig. 1 at the critical point that $g_c^\perp \approx 10^{-7} g_c^\parallel$, which is a much stronger variation than $g_c^\perp \approx t^2 g_c^\parallel$, predicted by the diagrammatic analysis⁹ of the anisotropic model and by the simple arguments presented in Ref. 19. The t^2 dependence of the ratio of the conductances is only correct in the weak scattering limit,¹⁹ where $g^\perp / g^\parallel \approx \xi^\parallel / \xi^\perp \approx t^2$. In general,

$$\begin{aligned} \frac{g^\perp}{g^\parallel} &= \frac{\exp(2L_\parallel / \lambda_M^\parallel) - 1}{\exp(2L_\perp / \lambda_M^\perp) - 1} = \frac{\exp(2L_\parallel \xi^\parallel / L_\perp^2) - 1}{\exp(2L_\perp \xi^\perp / L_\parallel^2) - 1} \\ &= \frac{\exp(2\xi^\parallel / L) - 1}{\exp(2\xi^\perp / L) - 1}. \end{aligned} \quad (9)$$

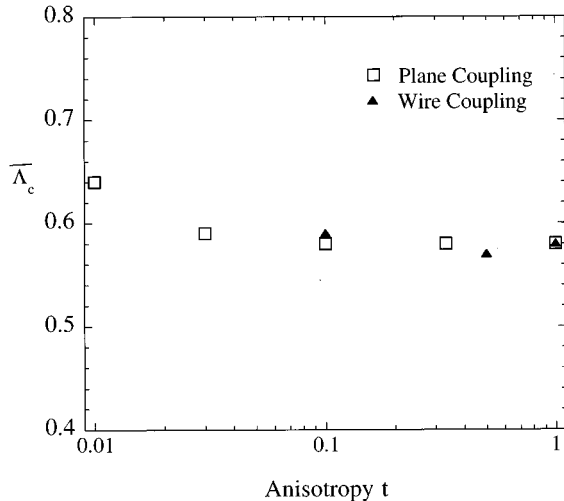


FIG. 5. Geometric mean value $\bar{\Lambda}_c = (\Lambda_c^x \Lambda_c^y \Lambda_c^z)^{1/3}$ vs the anisotropy t , for plane and wire coupling.

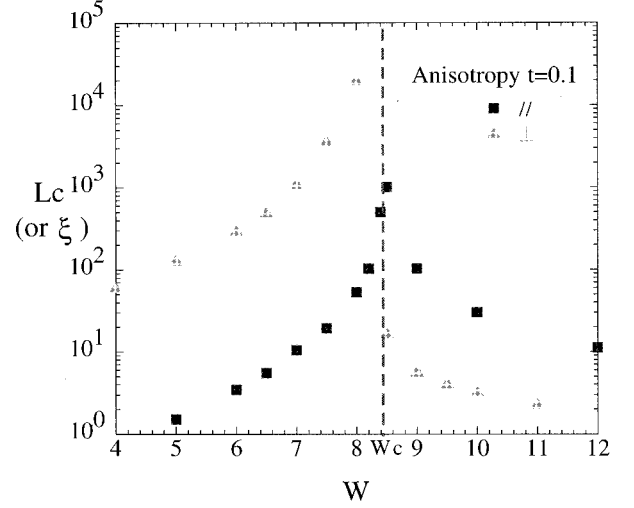


FIG. 6. Localization length L_c or correlation length ξ as a function of disorder W for $E=0$ and $t=0.1$, for the parallel and perpendicular propagating directions. Notice that for $W < W_c \approx 8.0$, $\xi^\perp > \xi^\parallel$, while for $W > W_c$, $L_c^\perp > L_c^\parallel$.

To obtain the last equality we have assumed that $L_\parallel = L_\perp = L = M$, as is the case for the numerical results of the conductance, where we used a cube of size $M \times M \times M$. Our numerical results of Fig. 6 have clearly shown that $\xi^\perp \gg \xi^\parallel$ is always correct for a strongly anisotropic system. We therefore have that if the size of the system $L \gg \xi^\perp \gg \xi^\parallel$, we can expand both the numerator and denominator of the last expression in Eq. (9) to obtain that indeed $g^\perp / g^\parallel \approx \xi^\parallel / \xi^\perp = t^2$. This is correct only in the weak disorder limit. Notice from Fig. 6 that even for weak disorder $W=2$, $\xi^\parallel \approx 1$, and $\xi^\perp \approx 20$, which is comparable to the maximum size used in our conductance calculations. If $\xi^\parallel \ll L \ll \xi^\perp$, Eq. (9) gives that $g^\perp / g^\parallel \approx (2\xi^\parallel / L) \exp(-2\xi^\perp / L)$, which is a much stronger dependence than t^2 . Similarly, if $L \ll \xi^\parallel \ll \xi^\perp$, Eq. (9) gives that $g^\perp / g^\parallel \approx \exp(-2\xi^\perp / L)$, which is also a much stronger dependence than the t^2 . This is the reason that $g_c^\perp \approx 10^{-7} g_c^\parallel$ at the critical point and *not* $g_c^\perp \approx t^2 g_c^\parallel$. Another point that is worth mentioning is that the geometric mean of the conductances of our anisotropic system is not equal to the critical conductance g_c of the isotropic system, which is roughly equal to 0.1 in units of e^2/h . Remember that the geometric mean of the critical λ_M / M is equal to a constant and is given by Eq. (8).

We have calculated the critical exponent ν for the localization length. This is done for the value $t=0.1$ for each of the propagating directions by utilizing the finite-size scaling ansatz [Eq. (5)]. We make the further assumption that the scaling parameter $\lambda(E, W)$ diverges as $W \rightarrow W_c$ from the localized side with a power law $(W - W_c)^{-\nu}$. We may then expand the function f

$$\frac{\lambda_M}{M} = A + BM^{\frac{1}{\nu}}(W - W_c) + O((W - W_c)^2), \quad (10)$$

where A and B are constants and

$$BM^{1/\nu} = \left. \frac{df}{dW} \right|_{W_c}. \quad (11)$$

TABLE I. Calculated values of ν , for propagation perpendicular to the planes, for different pairs (W_1, W_2) of the disorder W close to the mobility edge $W_c=8.25$.

W_1	W_2	ν
7.0	7.5	1.08
7.5	8.0	1.27
7.5	8.3	1.32
7.5	8.5	1.27
8.0	8.5	1.28
8.3	9.0	1.93
8.5	9.0	1.24

Therefore, ν is obtained as the reciprocal of the slope of the linear relationship between $\ln[df/dW]$ at $W=W_c$ and $\ln M$. For the numerical calculation of this slope we have used four values of M ($=11,13,15,17$) for the perpendicular propagating direction and three values of M ($=11,13,15$) for the parallel propagating direction. This is because for the parallel propagating direction the calculations up to $M=15$ are enough in order to have a correct estimation of the various quantities since there is a good linear scaling behavior of the λ_M/M vs M for $M \geq 11$. Actually, the calculation for $M=17$ needs really much CPU time and is at the limit of the available computers.

Numerically, we calculate the derivative df/dW using the values of λ_M/M for two neighbor values of W . For each pair of W 's we calculate a value of ν and finally we take the mean value of them to have an estimation of the ν exponent and the standard deviation as the error of the calculation $\Delta\nu$. In Table I we present the pairs of W 's (W_1, W_2) we used and the corresponding calculated values of ν for propagation perpendicular to the planes. The mean value of the ν 's gives an estimation of $\nu^\perp = 1.34$ and the standard deviation $\Delta\nu = 0.11$ gives an estimation of the error. Similarly, in Table II we present the pairs of W 's and the calculated values of ν for propagation parallel to the planes. The mean value of the ν 's gives an estimation of $\nu^\parallel = 1.31$ and the standard deviation gives an error $\Delta\nu = 0.21$. Within the numerical accuracy, the values $\nu^\perp = 1.3 \pm 0.1$ and $\nu^\parallel = 1.3 \pm 0.2$ are in agreement with the $\nu = 1.3 \pm 0.1$ for the isotropic system.

We have used the transfer-matrix and finite-scaling methods to obtain the mobility-edge trajectory for $t=0.1$ for all the values of E . This is shown in Fig. 7, where the strength of the critical disorder W_c versus E is shown for $t=0.1$.

TABLE II. Calculated values of ν , for propagation parallel to the planes, for different pairs (W_1, W_2) of the disorder W close to the mobility edge $W_c=8.25$.

W_1	W_2	ν
7.5	8.5	0.98
8.2	9.0	1.66
8.2	8.5	1.19
8.5	9.0	2.39
8.0	8.5	1.08
8.0	8.2	0.97
7.5	8.0	0.92

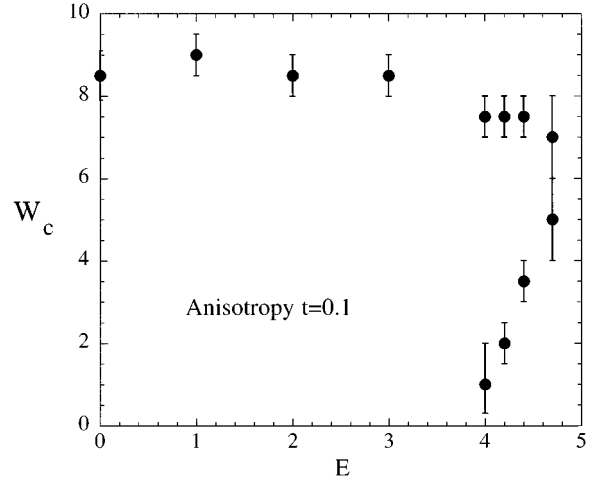


FIG. 7. Dependence of the mobility edge of the strength of the diagonal disorder W_c for anisotropy $t=0.1$.

Notice that the shape of the mobility-edge trajectory is similar to that of $t=1$ shown in Fig. 5 of Ref. 4. The $t=0.1$ trajectory plotted in Fig. 7 is a little different from the one shown in Fig. 5 of Ref. 4. In Ref. 4 the mobility-edge trajectory was obtained by assuming that $(\lambda_M/M)_c \approx 0.6$ for all t . We now know that this is not correct and therefore the correct mobility-edge trajectory is the one shown in Fig. 7 of the present paper. Notice that for $E=0$, $W_c=8.25$, while for $W \leq 1$, the mobility edge is at $E_c \approx 4.0$.

IV. TRANSPORT HIGH- T_c MATERIALS

The difference between ξ^\parallel and ξ^\perp is very important and can possibly explain the normal state transport properties⁶ of the high- T_c materials. The correlation length ξ measures the strength of the fluctuations of the wave functions in the extended regime. For length scales larger than ξ , the wave function looks uniform, while for length scales smaller than ξ , the wave function has strong fluctuations. Another relevant length scale is the inelastic mean free path l_{in} , which behaves as T^{-p} , with probably $p=1/2$. When $l_{in} < \xi$, a phenomenon called incipient localization takes place and conductivity is controlled by l_{in} . A convenient interpolation formula²⁰ valid in the conducting regime near the Anderson transition is given by

$$\sigma_{loc} = (e^2/\hbar)(\alpha/\xi + b/l_{in}), \quad (12)$$

where α and b are constants of order unity.¹⁹ For high enough temperatures the conductivity is given by the regular metallic behavior, where $\sigma_{ph} = \omega_p^2 \tau / 4\pi$ and the mean free time $\tau \sim T^{-1}$. Because σ_{ph} and σ_{loc} describe independent physical processes, we can add the corresponding resistivities. Therefore, $\rho = \rho_{loc} + \rho_{ph}$, where $\rho = 1/\sigma$. The experimental behavior of the high- T_c materials can be understood if we assume that the high- T_c oxides, instead of being insulators,⁷ are disordered anisotropic metals with a large anisotropic correlation length. At low T , the resistivity is dominant by ρ_{loc} . Once l_{in} becomes shorter than ξ in the perpendicular direction (c direction) ξ^\perp , Eq. (12) suggests

that there is a sharp downturn in the perpendicular resistivity as the temperature increases. This trend will eventually stop at some T when the regular resistivity begins to dominate. Then ρ^\perp will start increasing linearly with T , as in the regular metallic behavior. In the parallel direction ξ^\parallel is always smaller than the inelastic length and the transport in the plane remains metallic. The above analysis neglects corrections and dynamic disorder that could also substantially affect the transport properties.²

V. ANALYTICAL WORK

To study the behavior of the critical disorder W_c vs the anisotropy t we improved the analytical work using the coherent potential approximation (CPA) coupled with the potential well analogy (PWA) method, starting from the results of the diagrammatic analysis.⁹ The maximally crossed diagrams produced a correction to the zero-temperature configurationally average conductivity $\sigma_{i0}(i=x,y,z)$ of the form^{4,21}

$$\frac{\delta\sigma_i}{\sigma_{i0}} = \frac{e^2}{\pi\hbar} \frac{2}{(2\pi)^3} \int d\vec{k} \frac{1}{-i\omega[2e^2N(E)] + \sum_{k=1}^3 \sigma_{i0}k_i^2}, \quad (13)$$

where $\delta\sigma_i = \sigma_i - \sigma_{i0}$ and $N(E)$ is the density of states per unit cell per spin and the limit $\omega \rightarrow 0$ must be taken. In the weak scattering limit σ_{i0} is given^{21,22} by

$$\sigma_{i0} = \frac{e^2}{\hbar} \frac{1}{4\pi^3} S(E) \left\langle \frac{v_i^2}{v} \right\rangle \tau, \quad (14)$$

where τ is the isotropic relaxation time, v_i is the velocity in the i direction, $S(E)$ is the Fermi surface, and the average is taken over the surface $E(\vec{k}) = E$.

In a tight-binding model, the equivalent expression^{4,21} to Eq. (13) is

$$\begin{aligned} \frac{\delta\sigma_i}{\sigma_{i0}} = & - \frac{\Omega}{(2\pi)^3} \int d\vec{k} \\ & \times \frac{1}{-i\pi\hbar\omega\Omega N(E) + \sum_{i=1}^3 \frac{\pi\hbar\Omega}{e^2} \frac{\sigma_{i0}}{\alpha_i^2} [1 - \cos(k_i\alpha_i)]}, \end{aligned} \quad (15)$$

where we introduce a lattice constant α_i that depends on the i direction and $\Omega = \prod_{i=1}^3 \alpha_i$. It was found²² that α_i is proportional to the mean free path l_i and at this point we introduce the generalized assumption that the mean free path is different in different directions, i.e., the velocity v_i is taken to depend on the direction. The relaxation time τ is taken to be isotropic. Also, in our analysis we use the approximation

$$\alpha_i = C_1 l_i = C_1 [\langle v_i^2 \rangle]^{1/2} \tau \approx C_1 \left[\langle v \rangle \left\langle \frac{v_i^2}{v} \right\rangle \right]^{1/2} \tau, \quad (16)$$

where v is the velocity average over the surface $E(\vec{k}) = \text{const}$. Localization occurs when $\sigma_i(\omega \rightarrow 0) = 0$, i.e.,

$$\frac{\delta\sigma_i}{\sigma_{i0}} = -1 \Rightarrow 1 = \frac{1}{(2\pi)^3} \int d\vec{q} \frac{1}{\sum_{i=1}^3 \frac{\pi\hbar\Omega}{e^2} \frac{\sigma_{i0}}{\alpha_i^2} [1 - \cos q_i]} \quad (17)$$

in the tight-binding representation for the mobility edge. In the above we have defined $q_i = k_i \alpha_i$ as an effective momentum constant, which represents physically the upper momentum cutoff in the integral of Eq. (15).

Using relations (14) and (16) we derive that

$$\frac{\sigma_{i0}}{\alpha_i^2} = \frac{e^2}{\hbar} \frac{1}{4\pi^3} \frac{S(E)}{C_1^2 \tau \langle v \rangle}, \quad (18)$$

which is independent of i and therefore can be taken outside the summation over i in the denominator of Eq. (17). So the localization criterion (17) can be rewritten as

$$\frac{\pi\hbar\Omega\sigma_{i0}}{2e^2\alpha_i^2} = \frac{1}{(2\pi)^3} \int d\vec{q} \frac{1}{\sum_{i=1}^3 (2 - 2\cos q_i)} = G_{3D}^{is}(E=6), \quad (19)$$

where $G_{3D}^{is}(E=6) = 0.252731$ is the Green's function for the 3D isotropic simple cubic lattice, calculated at $E=6$ in units of V , the hopping integral.

A. Plane coupling

To describe a system of coupled planes, let us take the directions x and y to have hopping matrix elements $V=1$. Then $\alpha_x = \alpha_y$ and the localization criterion (19) becomes

$$\frac{\pi\hbar}{2e^2} \alpha_z \sigma_{x0} = G_{3D}^{is}(E=6) \quad (20)$$

or

$$\frac{1}{8\pi^2} C_1 \tau^2 S(E) \langle v \rangle^{1/2} \left\langle \frac{v_x^2}{v} \right\rangle \left\langle \frac{v_z^2}{v} \right\rangle^{1/2} = G_{3D}^{is}(E=6). \quad (21)$$

We define

$$t_e \equiv \frac{\sigma_{z0}}{\sigma_{x0}} = \frac{\left\langle \frac{v_z^2}{v} \right\rangle}{\left\langle \frac{v_x^2}{v} \right\rangle}, \quad (22)$$

so

$$\langle v \rangle = \left\langle \frac{v_x^2}{v} \right\rangle + \left\langle \frac{v_y^2}{v} \right\rangle + \left\langle \frac{v_z^2}{v} \right\rangle = \left\langle \frac{v_x^2}{v} \right\rangle (2 + t_e). \quad (23)$$

The quantity $S(E) \langle v_i^2/v \rangle$ can be expressed⁴ in terms of the lattice Green's functions, choosing the lattice constant α_0 as the unit of length, as

$$S(E) \left\langle \frac{v_x^2}{v} \right\rangle = \frac{4(2\pi)^2}{\hbar} t_x^2 [\text{Im}G(E;0,0,0) - \text{Im}G(E;2,0,0)] \quad (24)$$

and

$$S(E) \left\langle \frac{v_z^2}{v} \right\rangle = \frac{4(2\pi)^2}{\hbar} t_z^2 [\text{Im}G(E;0,0,0) - \text{Im}G(E;0,0,2)], \quad (25)$$

where G is the Green's function of the periodic anisotropic tight-binding system with hopping matrix elements ($t_x=1$, $t_y=1$, and $t_z=t$).

Combining Eqs. (21)–(23), we obtain an expression for the critical relaxation time τ_c for plane coupling

$$\tau_c^2 = \frac{8\pi^2 S(E) G_{3D}^{is}(E=6)}{C_1 [t_e(2+t_e)]^{1/2} \left(S(E) \left\langle \frac{v_x^2}{v} \right\rangle \right)^2} \quad (26)$$

and by the use of Eq. (24) we obtain that τ_c is equal to

$$\tau_c^2 = \frac{\hbar^2 S(E) G_{3D}^{is}(E=6)}{32\pi^2 C_1} \times \frac{1}{[t_e(2+t_e)]^{1/2} [\text{Im}G(E;0,0,0) - \text{Im}G(E;2,0,0)]^2}. \quad (27)$$

In Fig. 8(a) we plot the critical relaxation time τ_c vs the anisotropy t for coupled planes, as obtained from Eq. (27). To obtain τ_c we must know how $S(E=0)/C_1$ changes for different values of t . This is not easy, due to uncertainties in the value of C_1 . However, since $S(E=0)/C_1$ equals 6.75 for $t=1$ and 7.70 for $t=0$, we could have approximated it by its 3D value of $t=1$, but instead we have used that $S(E=0)/C_1 = 6.75[t + 1.141(1-t)]$. Notice that from the log-log plot of τ_c versus t [Fig. 8(a)] one clearly sees that the limiting behavior of τ_c , for small t , agrees very well with the results obtained from Eq. (32), that is, $\tau_c \sim t^{-1/2}$ as $t \rightarrow 0$.

In the limit of small coupling $t \rightarrow 0$ it can be shown⁴ that

$$\text{Im}G(0;0,0,0) \simeq \frac{2}{\pi} \ln 2 - \frac{1}{2\pi} \ln t, \quad (28)$$

$$\text{Im}G(0;0,0,2) \simeq -\frac{1}{4\pi}, \quad (29)$$

$$\text{Im}G(0;2,0,0) \simeq \frac{2}{\pi} (\ln 2 - 1) - \frac{1}{2\pi} \ln t, \quad (30)$$

so

$$t_e = t^2 \frac{[\text{Im}G(E;0,0,0) - \text{Im}G(E;0,0,2)]}{[\text{Im}G(E;0,0,0) - \text{Im}G(E;2,0,0)]} \simeq t^2 \left[\ln 2 + \frac{1}{8} - \frac{1}{4} \ln t \right]. \quad (31)$$

Using the above, we obtain $\tau_c \sim t^{-1/2}$,

$$\tau_c^2 \simeq \frac{\hbar^2 G_{3D}^{is}(E=6)}{128\sqrt{2} \left[\ln 2 + \frac{1}{8} \right]^{1/2}} \left(\frac{S(E)}{C_1} \right) \frac{1}{t} \quad (32)$$

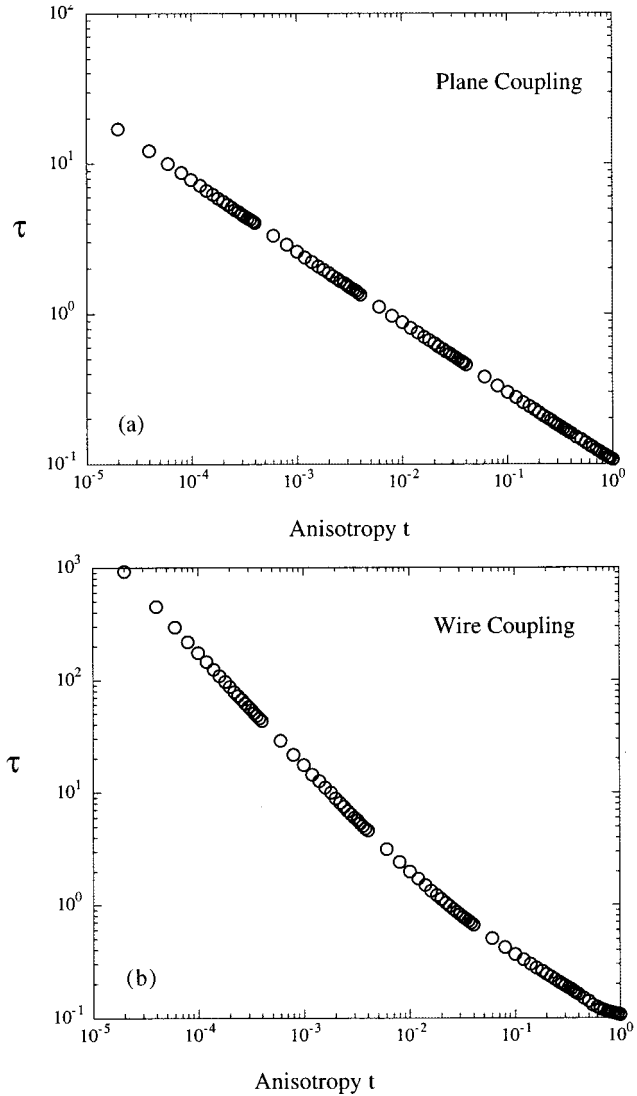


FIG. 8. Critical relaxation time τ_c vs the anisotropy t for (a) weakly coupled planes and (b) weakly coupled wires.

and by using that $S(E)/C_1 \simeq 7.70$, its $t=0$ value, we obtain that

$$\tau = \frac{0.109\hbar}{t^{1/2}}. \quad (33)$$

Taking into account that $\tau \sim W^{-2}$ in the weak scattering limit, we obtain the limiting behavior $W_c \sim t^{1/4}$ as $t \rightarrow 0$ for weakly coupled planes.

In previous analytical work,⁴ the critical relaxation time τ_c vs the anisotropy t for coupled planes has been obtained, but using the same mean free path in all directions. This analysis gives that $W_c \sim 1/\sqrt{|\ln t|}$ when $t \rightarrow 0$, which is drastically different from our present result $W_c \sim t^{1/4}$. It must be stressed that in isotropic systems it is accepted that the cutoff length α is proportional to l . However, in anisotropic systems it is not *a priori* clear whether $\alpha_i = C_1 l_i$ or $\alpha_i = C_2 l$, where l is an appropriate average of the l_i 's. The present numerical data seem to support the choice $\alpha_i = C_1 l_i$.

B. Wire coupling

To describe a system of weakly coupled chains we define the hopping matrix elements as $(t_x, t_y, t_z) = (t, t, 1)$, i.e., the z direction is chosen as the large hopping direction. We define

$$t_e \equiv \frac{\sigma_{x0}}{\sigma_{z0}} = \frac{\left\langle \frac{v_x^2}{v} \right\rangle}{\left\langle \frac{v_z^2}{v} \right\rangle} = t^2 \frac{[\text{Im}G(E;0,0,0) - \text{Im}G(E;2,0,0)]}{[\text{Im}G(E;0,0,0) - \text{Im}G(E;0,0,2)]}. \quad (34)$$

In this case, $\alpha_x = \alpha_z$ and the localization criterion (19) becomes

$$\frac{\pi \hbar}{2e^2} \alpha_z \sigma_{x0} = G_{3D}^{is}(E=6). \quad (35)$$

Using that

$$\left\langle \frac{v_x^2}{v} \right\rangle = t_e \left\langle \frac{v_z^2}{v} \right\rangle = \frac{t_e}{1+2t_e} \langle v \rangle \quad (36)$$

and Eqs. (14), (16), (34), and (35), we obtain that

$$\tau_c^2 = \frac{\hbar^2 S(E) G_{3D}^{is}(E=6)}{32\pi^2 C_1} \times \frac{1}{t_e(1+2t_e)^{1/2} [\text{Im}G(E;0,0,0) - \text{Im}G(E;0,0,2)]^2}. \quad (37)$$

In Fig. 8(b) we plot the behavior of the critical relaxation time τ_c as a function of anisotropy strength t for weakly coupled wires. τ_c is calculated using Eq. (37). To obtain τ_c , we must know how $S(E=0)/C_1$ changes for different values of t . As we have mentioned above, this is not easy, due to uncertainties in the value of C_1 . However, since $S(E=0)/C_1$ equals 6.75 for $t=1$ and $1/\pi$ for $t=0$, we have used that $S(E=0)/C_1 = 6.75[t + (1/6.75\pi)(1-t)]$ for all values of t . Notice that the limiting behavior of τ_c , for small t , is given by $\tau_c \sim 1/t$ and agrees very well with the results obtained from Eqs. (37) and (40).

In the limit of weak wire coupling $t \rightarrow 0$ it can be shown²¹ that

$$\text{Im}G(E;0,0,0) - \text{Im}G(E;0,0,2) \approx -1, \quad (38)$$

$$\text{Im}G(E;0,0,0) - \text{Im}G(E;2,0,0) \approx -\frac{1}{2}, \quad (39)$$

so

$$t_e \approx \frac{1}{2} t^2 \Rightarrow \tau_c \sim \frac{1}{t}. \quad (40)$$

Using Eqs. (37)–(40), we obtain that the limit $t \rightarrow 0$ of Eq. (37) is given by

$$\tau_c^2 = \frac{\hbar^2 G_{3D}^{is}(E=6)}{16\pi^2} \frac{S(E)}{C_1} \frac{1}{t^2} \quad (41)$$

and by using that $S(E)/C_1 \approx 1/\pi$, its $t=0$ value, we obtain that

$$\tau_c = \frac{0.0226\hbar}{t}. \quad (42)$$

Taking into account that $\tau \sim W^{-2}$ in the weak scattering limit, we obtain the limiting behavior $W_c \sim t^{1/2}$ as $t \rightarrow 0$ for weakly coupled lines. In previous analytical work,²³ where the same mean free path in all directions was used, the limit of the critical relaxation time τ_c for weak coupling ($t \rightarrow 0$) is the same as the limit in the present work $\tau_c \sim 1/t$, although the full expression for τ_c is different.

C. CPA and results

The relaxation time τ for a disordered system can be calculated through the CPA by utilizing the relation

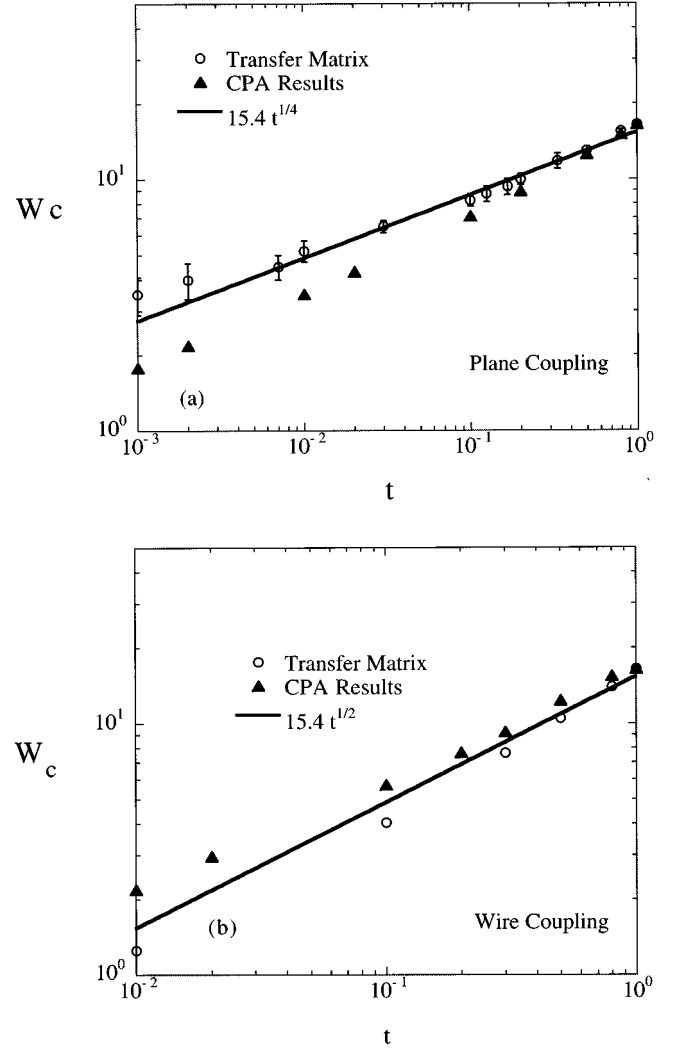


FIG. 9. Critical disorder W_c for localization vs the anisotropy t for (a) plane and (b) wire coupling. Open circles are results calculated through the CPA method and solid triangles are the numerical results calculated by transfer matrix techniques.

$$\tau = \frac{0.5\hbar}{\text{Im}\Sigma}, \quad (43)$$

where Σ is the CPA self-energy obtained by solving the self-consistent²² equation

$$\Sigma = \left\langle \frac{\varepsilon_n}{1 - (\varepsilon_n - \Sigma)G(E - \Sigma)} \right\rangle. \quad (44)$$

For $E=0$, the solution Σ of this equation has no real part. Hence no shift in energy is taking place. For simplicity, we will concentrate on the band center $E=0$. In Eq. (44) the site energies ε_n take values from a rectangular distribution of width W . The critical disorder W_c in which the transition of extended to localized states occur is the value of disorder, which in Eq. (43) gives a relaxation time equal to the critical value τ_c [which is known from Eq. (27) for plane coupling or Eq. (37) for wire coupling].

Using the above procedure, we obtained the critical disorder W_c for some values of t for plane and wire coupling. We compare those values with the numerical results obtained using the transfer-matrix method and finite-size scaling techniques, in Figs. 9(a) and 9(b). In Fig. 9(a) we plot W_c as a function of anisotropy t for the weakly coupled planes. Notice that our predictions of our anisotropic CPA, shown as solid triangles, are in agreement with the transfer-matrix results, which are shown as open circles. The CPA results of W_c can be fitted well with a single power-law dependence $W_c \approx 15.4t^{1/4}$ for $t < 0.8$. The numerical results (solid triangles) are larger than the CPA results for $t \leq 0.1$ and they do not drop as fast as the CPA results for $t \leq 0.2$. We want to stress that the numerical results for W_c are very difficult to obtain for $t \leq 0.2$ and it is possible that larger errors might be found. However, both our numerical results and the CPA results show a power-law dependence of W_c vs t . Most probably $W_c \sim t^{1/4}$. This dependence is in marked contrast to what one would expect based on a reasonable heuristic argument²⁴ and also predicted previously by more elaborate theories,^{1,4} which give a much weaker t dependence $W_c \sim 1/\sqrt{|\ln t|}$. The t dependence is also different from the results obtained for the weakly coupled chains,²² which give $W_c \sim t^{1/2}$; we will discuss this below. As we have argued above in Eq. (16), the reason for $W_c \sim t^{1/4}$ is that in an anisotropic system the effective lattice constant α_i has to be proportional to an anisotropic mean free path l_i . We believe that this choice may be

the proper one and the good agreement of our numerical results with $W_c \sim t^{1/4}$ provides further support to this choice.

In Fig. 9(b) we plot W_c as a function of anisotropy t for the weakly coupled chains. Notice that the predictions of our anisotropic CPA, shown as solid triangles, are in agreement with our transfer-matrix results, which are shown as open circles. The CPA results of W_c vs t can be fitted well with a single power-law dependence $W_c \approx 15.4t^{1/2}$ for $t < 0.8$. The numerical results (open circles) are in excellent agreement with the CPA results.

VI. CONCLUSION

In this work we have numerically and analytically studied highly anisotropic systems that represent weakly coupled planes and weakly coupled wires. For the numerical study we used the transfer-matrix techniques, while for the analytical study we used the self-consistent theory of localization represented by the PWA with the CPA. Numerically we found that there is only one mobility edge for both propagating directions, i.e., the states in the direction parallel to the planes (or wires) became localized at exactly the same amount of disorder as the states in the perpendicular direction. However, the correlation length ξ of the extended side of the transition and the localization length of the localized side can be very different for the two propagating directions. This behavior of ξ can possibly explain the transport properties of high- T_c materials. The critical value of disorder W_c seems to be proportional to $t^{1/4}$ for weakly coupled planes and is proportional to $t^{1/2}$ for weakly coupled chains, as obtained from our analytical investigations, assuming that the effective cutoff α_i is proportional to the corresponding mean free path l_i for each direction.

ACKNOWLEDGMENTS

We are grateful to Dr. Rojo for sending us his numerical data at the early stage of the project. Ames Laboratory is operated for the U.S. Department of Energy by Iowa State University under Contract No. W-7405-ENG-82. This work was supported by the Director of Energy Research, Office of Basic Energy Sciences and NATO Grant No. CRG 940647. It was also supported by EU Grant No. ERBFMBIC-CT96-0640 and a ΠENEΔ Research Grant at the Greek Secretariat of Science and Technology.

¹A. A. Abrikosov, Phys. Rev. B **50**, 1415 (1994).

²A. G. Rojo and K. Levin, Phys. Rev. B **48**, 16 861 (1993), and references therein.

³Y. Zha, S. L. Cooper, and D. Pines, J. Phys. Chem. Solids **56**, 1781 (1995); Y. Zha, Philos. Mag. B **74**, 497 (1996).

⁴Qiming Li, C. M. Soukoulis, E. N. Economou, and G. S. Grest, Phys. Rev. B **40**, 2825 (1989).

⁵W. Xue, P. Sheng, Q. J. Chu, and Z. Q. Zhang, Phys. Rev. Lett. **63**, 2837 (1989); Z. Q. Zhang, Q. J. Chu, W. Xue, and P. Sheng, Phys. Rev. B **42**, 4613 (1990); Q. J. Chu and Z. Q. Zhang, *ibid.* **48**, 10 761 (1993).

⁶For a review of experiments see Y. Iye, in *Physical Properties of*

High T_c superconductors, edited by D. M. Ginzberg (World Scientific, Singapore, 1992).

⁷G. Kotliar *et al.*, Europhys. Lett. **15**, 655 (1991).

⁸For a recent review, see B. Kramer and A. MacKinnon, Rep. Prog. Phys. **56**, 1469 (1993).

⁹P. Wölfle and R. N. Bhatt, Phys. Rev. B **30**, 3542 (1984); R. N. Bhatt, P. Wölfle, and T. V. Ramakrishnan, *ibid.* **32**, 569 (1985).

¹⁰W. Apel and T. M. Rice, J. Phys. C **16**, L1151 (1983).

¹¹I. Zambetaki, Qiming Li, E. N. Economou, and C. M. Soukoulis, Phys. Rev. Lett. **76**, 3614 (1996).

¹²J.-L. Pichard and G. Sarma, J. Phys. C **14**, L617 (1981); J. T. Chalker and P. D. Coddington, *ibid.* **21** 2665 (1988); M. Hen-

- kel, J. Phys. A **20**, L769 (1987).
- ¹³Qiming Li and C. M. Soukoulis (unpublished).
- ¹⁴For a discussion of the two methods see J.-L. Pichard, N. Zanon, Y. Imry, and A. D. Stone, J. Phys. (France) **51**, 587 (1990).
- ¹⁵V. I. Oseledec, Trans. Moscow Math. Soc. **19**, 197 (1968).
- ¹⁶J.-L. Pichard, Ph.D. thesis, Université de Paris Orsay, 1984; J.-L. Pichard and André, Europhys. Lett. **2**, 477 (1986).
- ¹⁷E. N. Economou and C. M. Soukoulis, Phys. Rev. Lett. **46**, 618 (1981); D. S. Fisher and P. A. Lee, Phys. Rev. B **23**, 6851 (1981).
- ¹⁸Qiming Li, S. Katsoprinakis, E. N. Economou, and C. M. Soukoulis, Phys. Rev. B **56**, R4297 (1997).
- ¹⁹The relation $g \approx 1/[\exp(2L\gamma/\lambda_M) - 1]$ [Eq. (1)] has been derived [E. N. Economou *et al.*, Phys. Rev. B **31**, 6485 (1985)] using Anderson's argument [P. W. Anderson, *ibid.* **23**, 4828 (1981)] that a well-behaved quantity that can serve as a single scaling parameter and is also additive with respect to the length L is the ratio $\gamma L/\lambda_M$, where γ is a slowly varying function of L/λ_M . It was found numerically that γ varies between 1.13 and 1 as L/λ_M varies from infinity to much less than unity. Thus γ can be taken to be 1 in Eq. (1). The above derivation of Eq. (1) is based also upon the double inequality $l, 1 \ll M \ll \lambda_M$, where $M \times M$ is the cross section of the bar of length L and mean free path l . Thus Eq. (1) is certainly not valid in the ballistic regime where $l \geq M$ or $l \geq L$. However, it is valid in the weak scattering (but not ballistic) regime $l \ll M, L$ and $l \ll \lambda_M$ (in this regime $\lambda_M \approx M^2/\xi$, $\xi \approx 1/l$, and thus the double inequality $l \ll M, L \ll \lambda_M$ is easily satisfied). It is worthwhile to point out that numerical calculations show that Eq. (1) works even near the critical regime (where $\xi \rightarrow \infty$) in spite of the breakdown of the inequality $M \ll \lambda_M$. In the weak disorder limit $\lambda_M \gg M$, the dimensionless conductance $g \sim 1/[\exp(2M/\lambda_M) - 1]$ can be expanded and gives that $g \sim \lambda_M/M$. By using the data of Fig. 2, which obey Eq. (6), we obtain that $g \sim \alpha + M/\xi$ and therefore $\sigma = g/M \sim \alpha/M + 1/\xi$, where ξ is the correlation length. The coefficient α is approximately a constant of order Λ_c away from the critical point. Notice that $\Lambda_c^\parallel = 1.2$ and $\Lambda_c^\perp = 0.12$ for $t = 0.1$. For the infinite-size system $M \rightarrow \infty$, $\sigma \sim 1/\xi$, and therefore $\sigma^\parallel/\sigma^\perp = \xi^\perp/\xi^\parallel$. In the weak disorder limit $\sigma^\perp/\sigma^\parallel \sim t^2$ and therefore $\xi^\parallel = t^2 \xi^\perp$. The ratio of the localization lengths can be obtained by using the length rescaling idea. The conductances in all the directions are the same if the dimension of the system is proportional to the localization length in that direction. This implies the expression $L_c^\perp/L_c^\parallel = (\sigma^\perp/\sigma^\parallel)^{1/2}$ and since $\sigma^\perp \sim t^2 \sigma^\parallel$, we obtain that $L_c^\perp = t L_c^\parallel$.
- ²⁰Y. Imry, Phys. Rev. Lett. **44**, 469 (1980); J. Appl. Phys. **52**, 1817 (1981); M. Jonson and S. M. Girvin, Phys. Rev. Lett. **43**, 1447 (1979); S. M. Girvin and M. Jonson, Phys. Rev. B **22**, 3583 (1980).
- ²¹E. N. Economou, *Green's Functions in Quantum Physics*, 2nd ed. (Springer, Heidelberg, 1983).
- ²²E. N. Economou and C. M. Soukoulis, Phys. Rev. B **28**, 1093 (1983); E. N. Economou, C. M. Soukoulis, and A. D. Zdetsis, *ibid.* **30**, 1686 (1984).
- ²³N. A. Panagiotides, S. N. Evangelou, and G. Theodorou, Phys. Rev. B **49**, 14 122 (1994); O. N. Dorokhor, Solid State Commun. **46**, 605 (1983); **51**, 381 (1984).
- ²⁴To determine the critical disorder W_c where the system crosses over from one to three dimensions for the weakly coupled chains and from two to three dimensions for the weakly coupled planes we consider a particle in a particular chain or plane, respectively. With probability $1/2(3-d)$ the particle will hop to another chain or plane after a time and therefore distance proportional to $1/t$, where t is hopping integral. The localization length L_c in the 1D [2D] case is proportional to $1/W^2$ [$\exp(\alpha/W^2)$], respectively. So the condition $L_c \approx 1/t$ determines the critical disorder W_c . For the one to three dimensions, we have $1/W_c^2 \approx 1/t$ and therefore $W_c \sim t^{1/2}$. For two to three dimensions, we have $\exp(\alpha/W_c^2) \approx 1/t$ and therefore $W_c \sim 1/\sqrt{|\ln t|}$.